A) Histograms

Dihedral $C_2C_1C_6C_7$

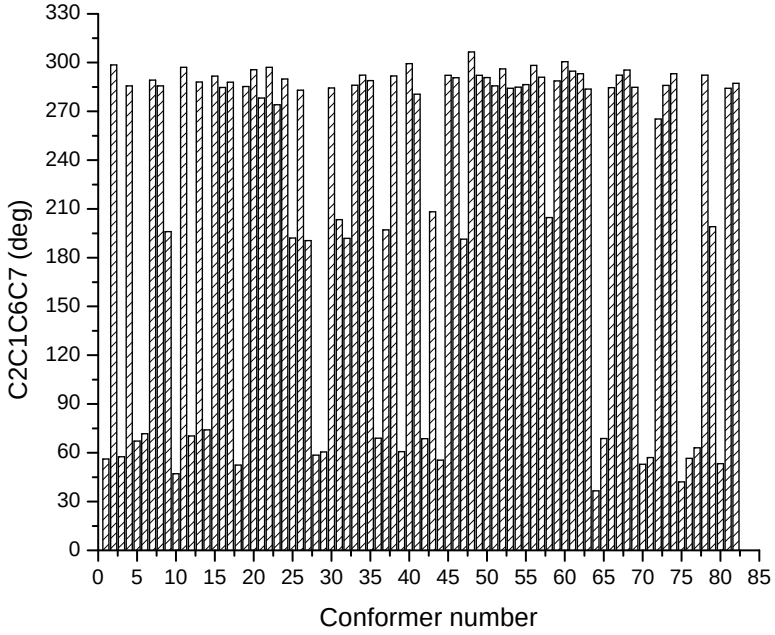

Fig.1. Values of the $C_2C_1C_6C_7$ dihedral in 82 PM3 conformers of PGE2 in a range of 3 kcal/mol

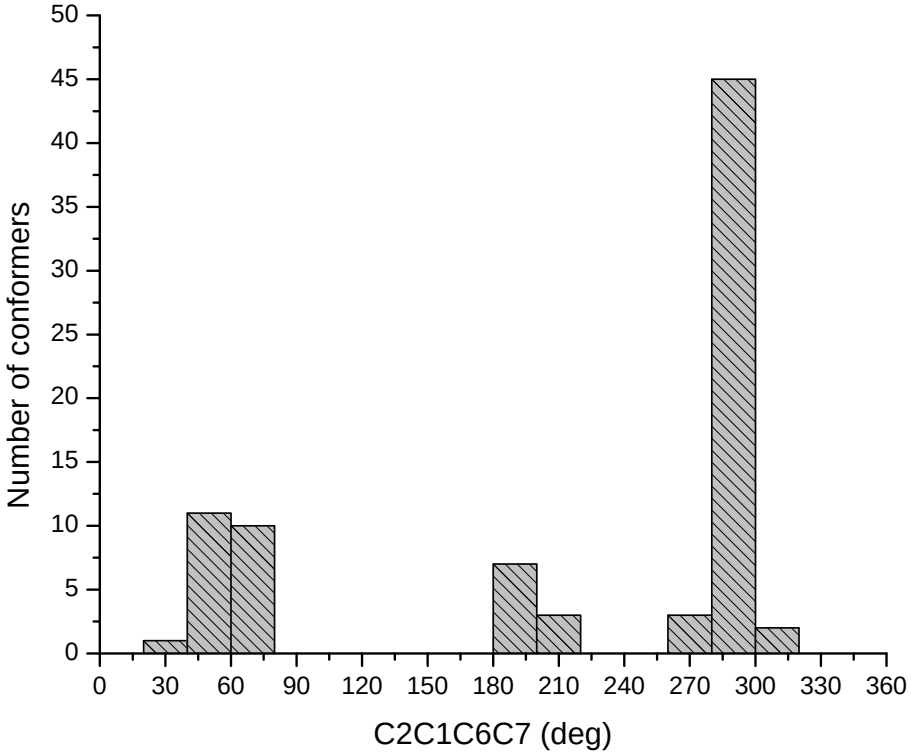

Fig.2. Histogram of the $C_2C_1C_6C_7$ dihedral values in 82 PM3 conformers of PGE2 in a range of 3 kcal/mol

Dihedral $C_1C_6C_7C_8$

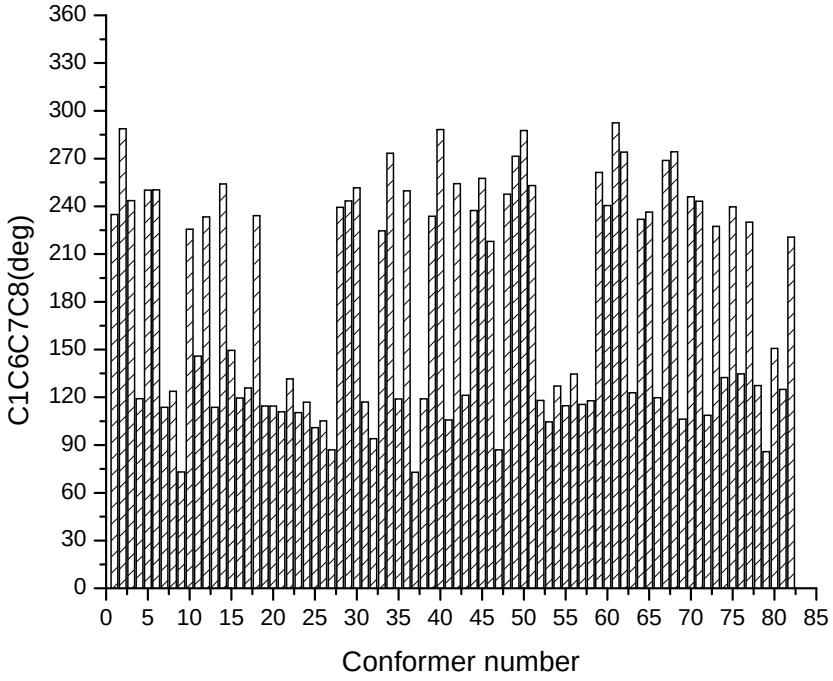

Fig. 3. Values of the $C_1C_6C_7C_8$ dihedral in 82 conformers of PM3 PGE2 in a range of 3 kcal/mol

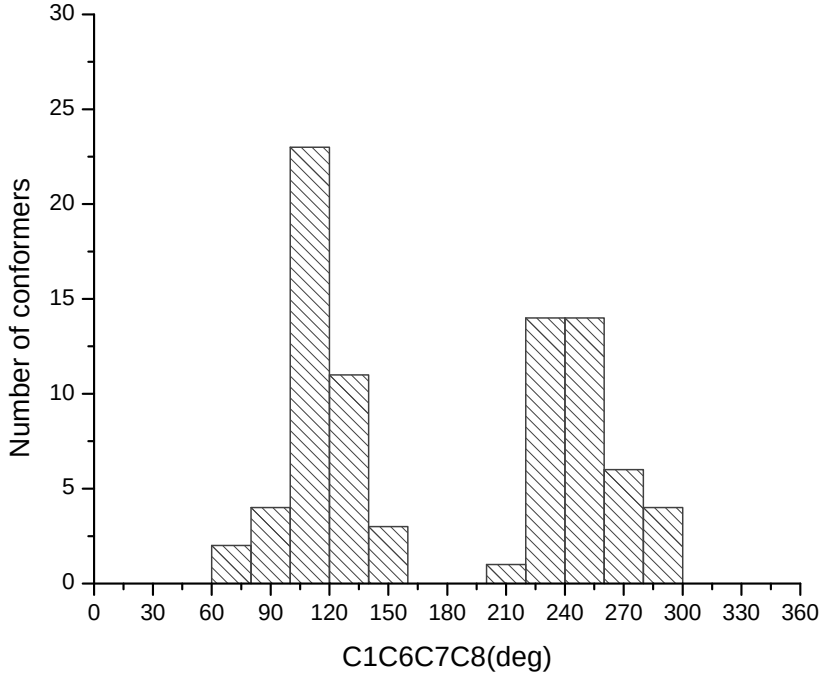

Fig.4. Histogram of the $C_2C_1C_6C_7$ dihedral values in 82 PM3 conformers of PGE2 in a range of 3 kcal/mol

Dihedral $C_7C_8C_9C_{10}$

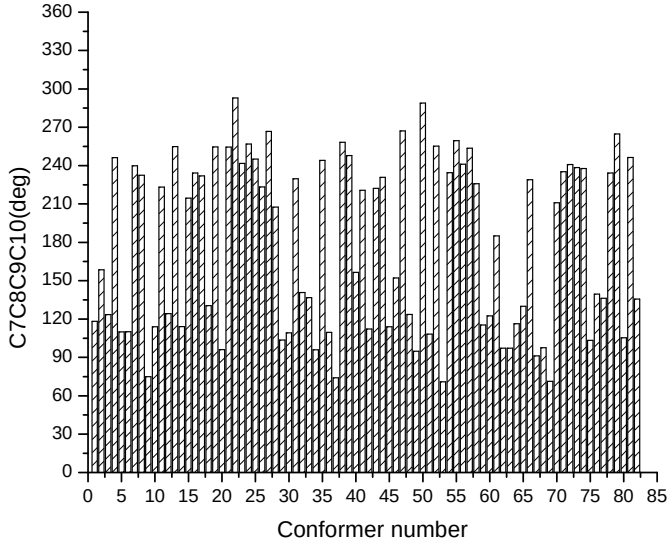

Fig.5. Values of the $C_7C_8C_9C_{10}$ dihedral in 82 PM3 conformers of PGE2 in a range of 3 kcal/mol

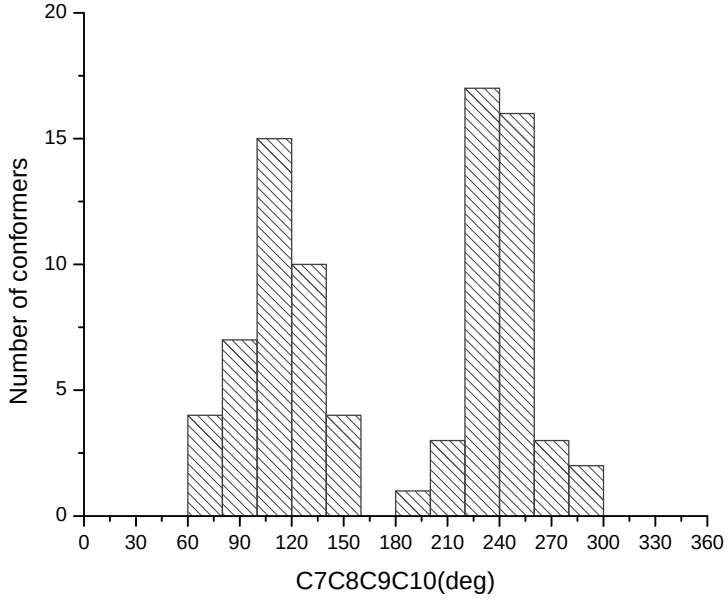

Fig. 6. Histogram of the $C_7C_8C_9C_{10}$ dihedral values in 82 PM3 conformers of PGE2 in a range of 3 kcal/mol

Dihedral $C_8C_9C_{10}C_{11}$

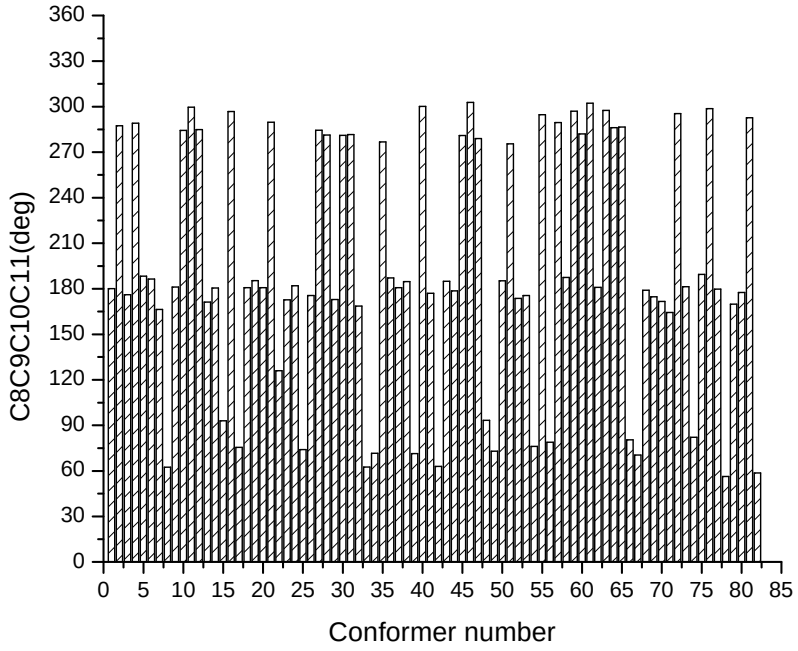

Fig. 7. Values of the $C_8C_9C_{10}C_{11}$ dihedral in 82 PM3 conformers of PGE2 in a range of 3 kcal/mol

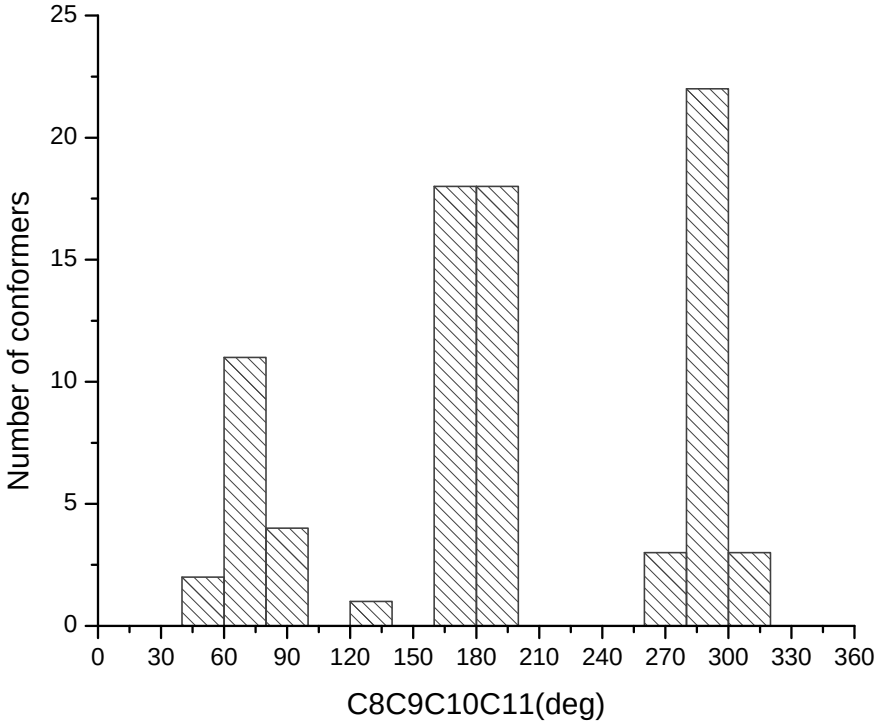

Fig. 8. Histogram of the $C_8C_9C_{10}C_{11}$ dihedral values in 82 PM3 conformers of PGE2 in a range of 3 kcal/mol

Dihedral $C_9C_{10}C_{11}C_{12}$

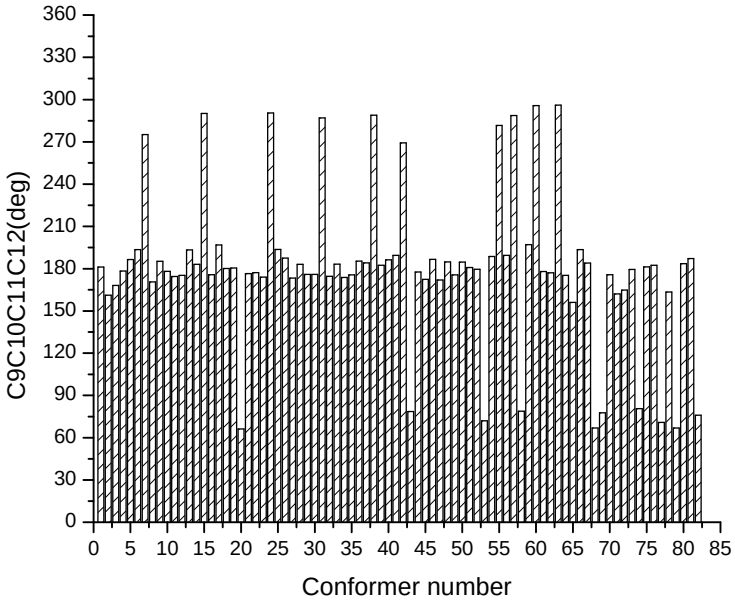

Fig. 9. Values of the $C_9C_{10}C_{11}C_{12}$ dihedral in 82 PM3 conformers of PGE2 in a range of 3 kcal/mol

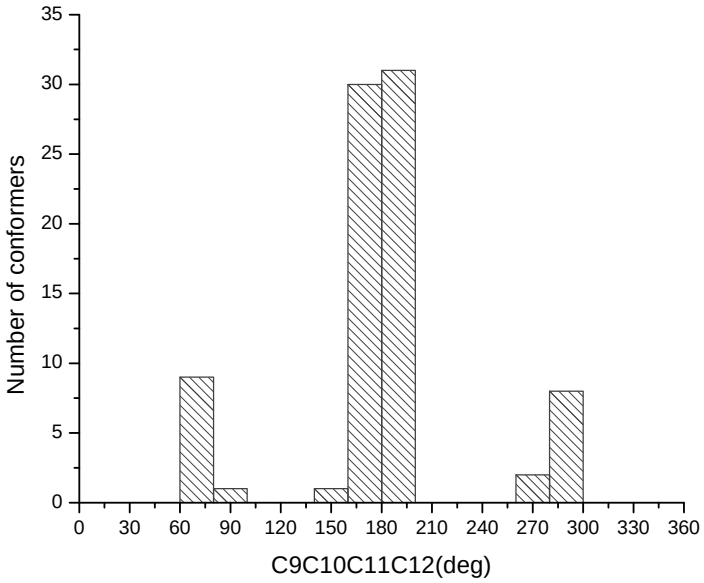

Fig.10. Histogram of the $C_9C_{10}C_{11}C_{12}$ dihedral values in 82 OM3 conformers of PGE2 in a range of 3 kcal/mol

Diehdral $C_{10}C_{11}C_{12}O_{14}$

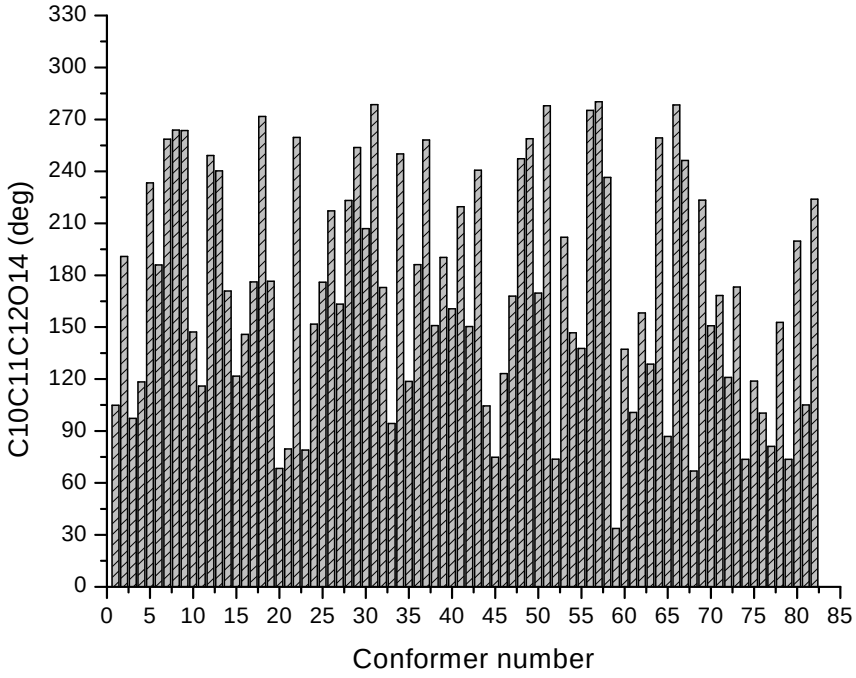

Fig. 11. Values of the $C_{10}C_{11}C_{12}O_{14}$ dihedral in 82 PM3 conformers of PGE2 in a range of 3 kcal/mol

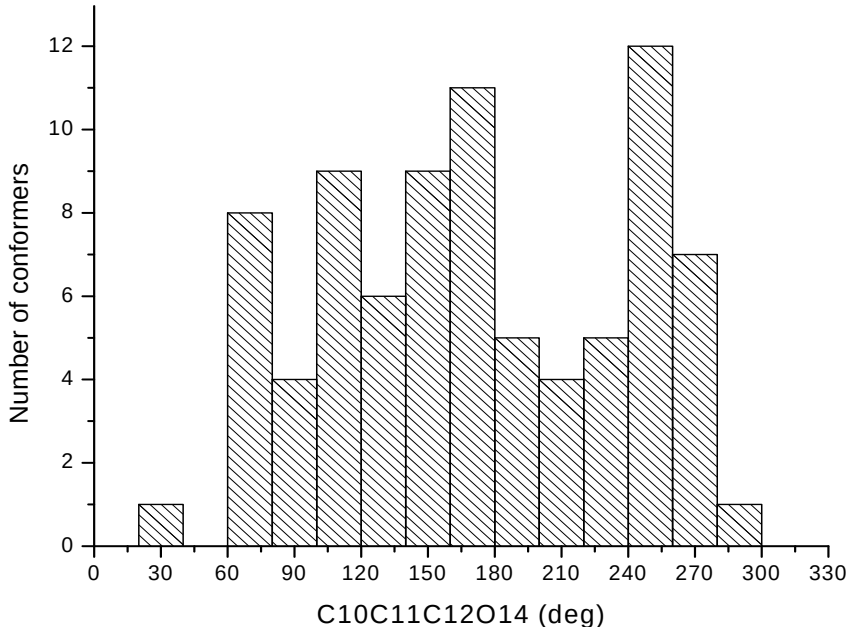

Fig.12. Histogram of the $C_{10}C_{11}C_{12}O_{14}$ dihedral values in 82 PM3 conformers of PGE2 in a range of 3 kcal/mol

Dihedral $C_1C_2C_{15}C_{16}$

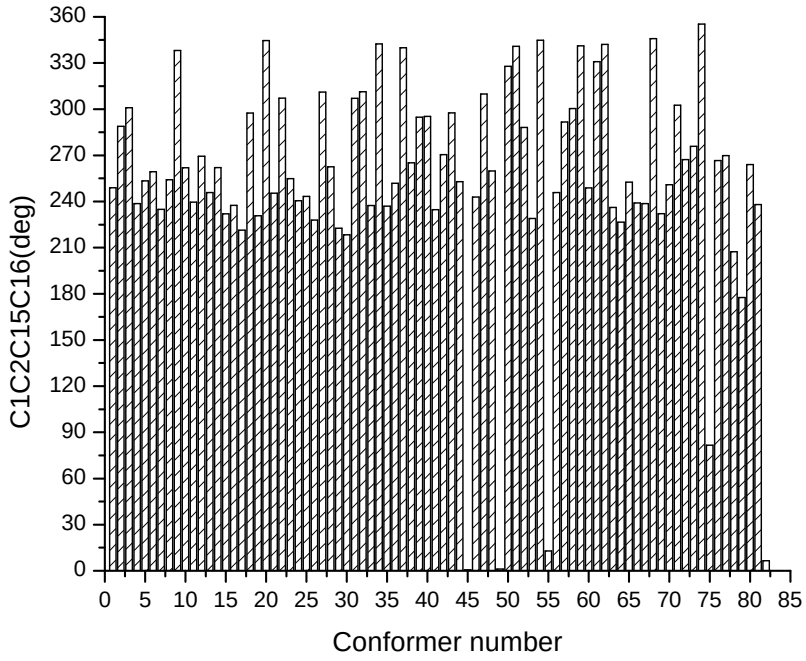

Fig.13. Values of the $C_1C_2C_{15}C_{16}$ dihedral in 82 PM3 conformers of PGE2 in a range of 3 kcal/mol

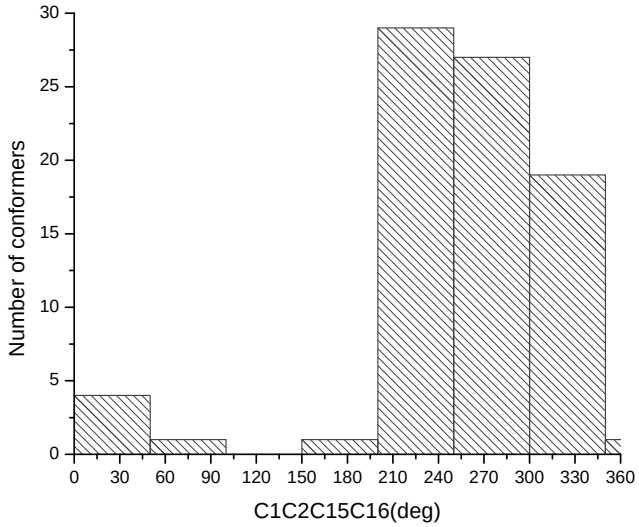

Fig. 14. Histogram of the $C_1C_2C_{15}C_{16}$ dihedral values in 82 PM3 conformers of PGE2 in a range of 3 kcal/mol

Dihedral $C_{15}C_{16}C_{17}C_{19}$

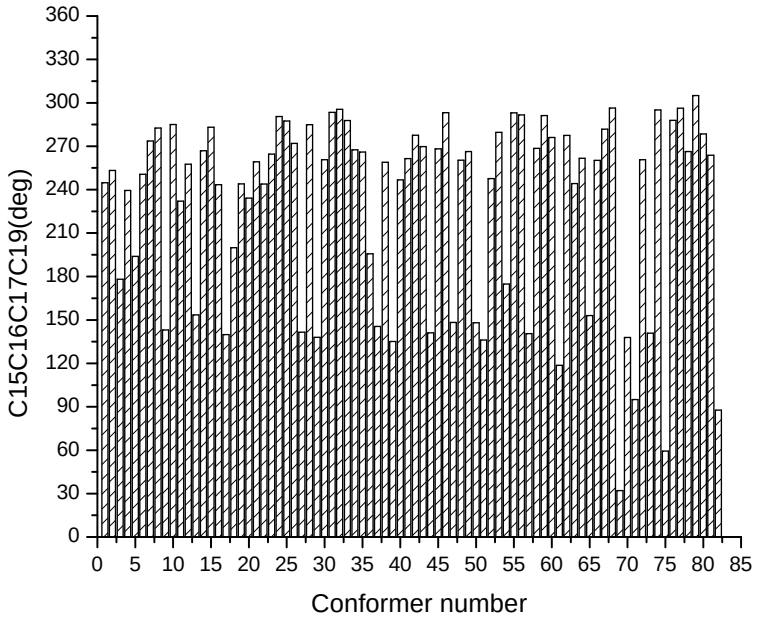

Fig. 15. Values of the $C_{15}C_{16}C_{17}C_{19}$ dihedral in 82 PM3 conformers of PGE2 in a range of 3 kcal/mol

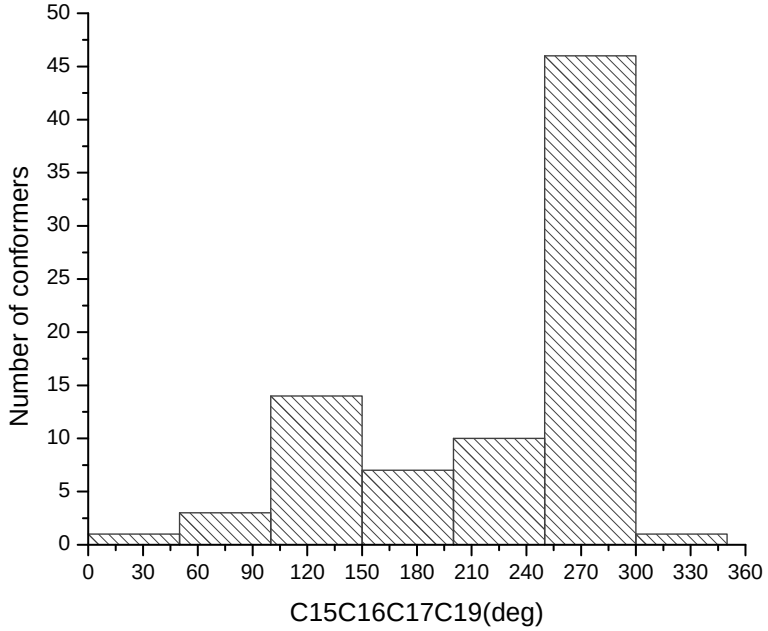

Fig.16. Histogram of the $C_{15}C_{16}C_{17}C_{19}$ dihedral values in 82 PM3 conformers of PGE2 in a range of 3 kcal/mol

Dihedral $C_{16}C_{17}C_{19}C_{20}$

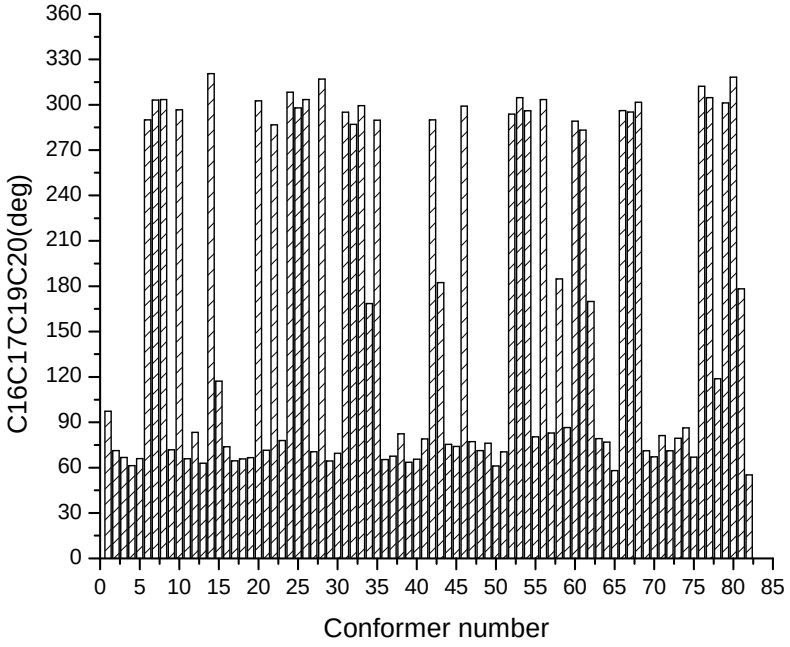

Fig.17. Values of the $C_{16}C_{17}C_{19}C_{20}$ dihedral in 82 PM3 conformers of PGE2 in a range of 3 kcal/mol

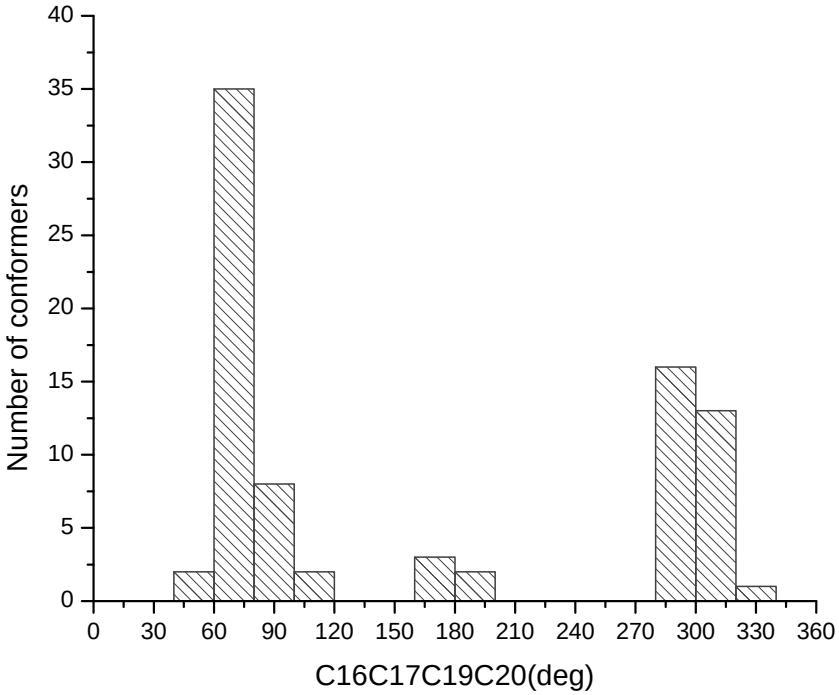

Fig. 18. Histogram of the $C_{16}C_{17}C_{19}C_{20}$ dihedral values in 82 PM3 conformers of PGE2 in a range of 3 kcal/mol

Dihedral $C_{16}C_{17}O_{18}H_{45}$

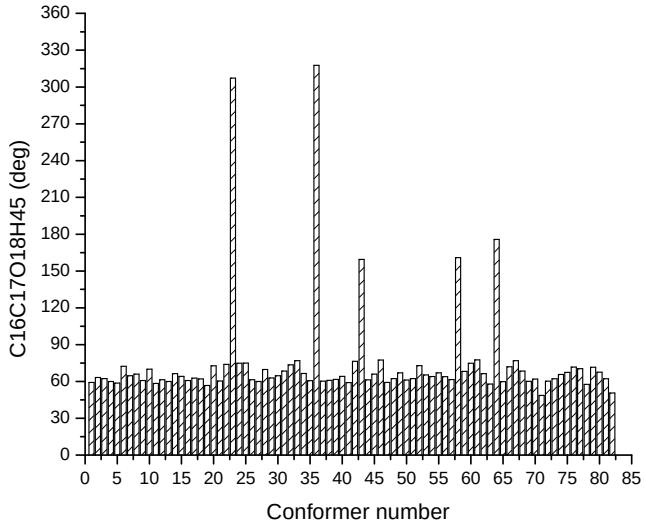

Fig. 19. Values of the $C_{16}C_{17}O_{18}H_{45}$ dihedral in 82 PM3 conformers of PGE2 in a range of 3 kcal/mol

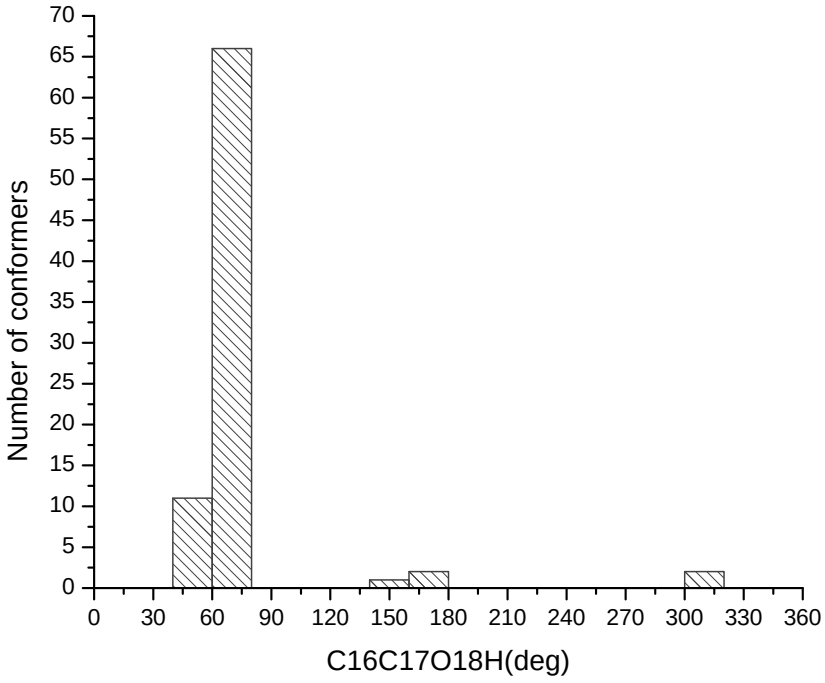

Fig. 20. Histogram of the $C_{16}C_{17}O_{18}H_{45}$ dihedral values in 82 PM3 conformers of PGE2 in a range of 3 kcal/mol

Dihedral $C_{17}C_{19}C_{20}C_{21}$

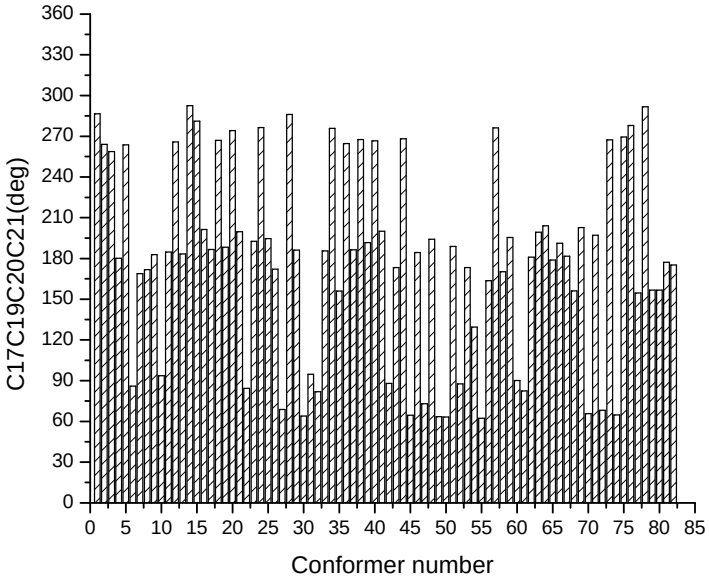

Fig. 21. Values of the $C_{17}C_{19}C_{20}C_{21}$ dihedral in 82 PM3 conformers of PGE2 in a range of 3 kcal/mol

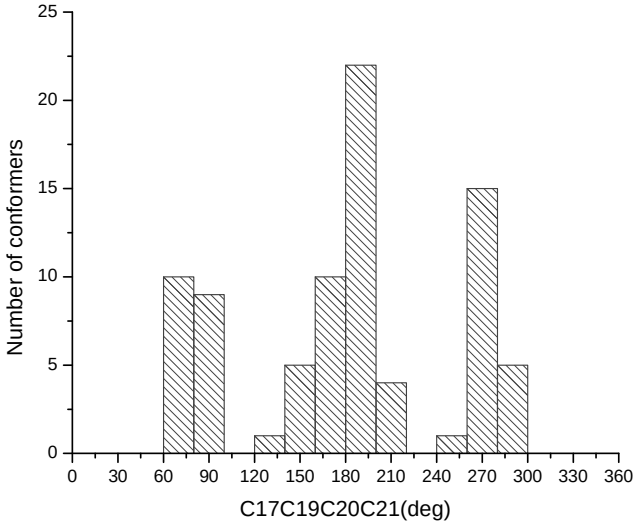

Fig.22. Histogram of the $C_{17}C_{19}C_{20}C_{21}$ dihedral values in 82 PM3 conformers of PGE2 in a range of 3 kcal/mol

Dihedral $C_{19}C_{20}C_{21}C_{22}$

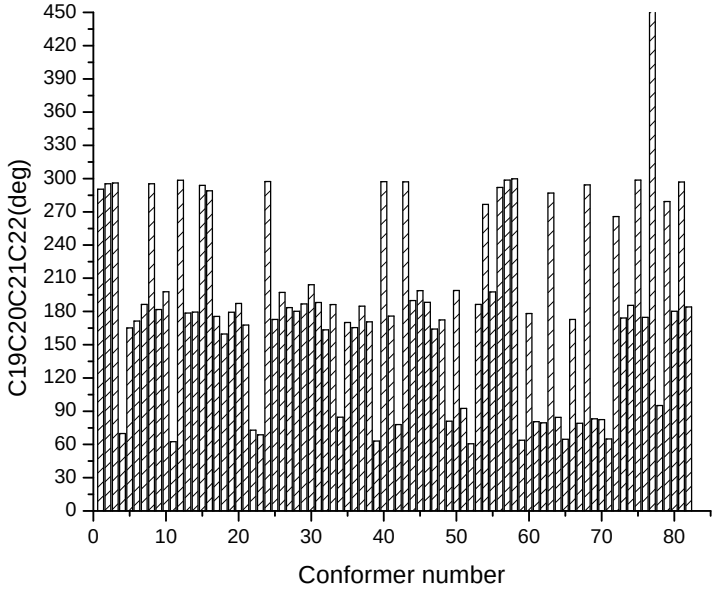

Fig. 23. Values of the $C_{19}C_{20}C_{21}C_{22}$ dihedral in 82 PM3 conformers of PGE2 in a range of 3 kcal/mol

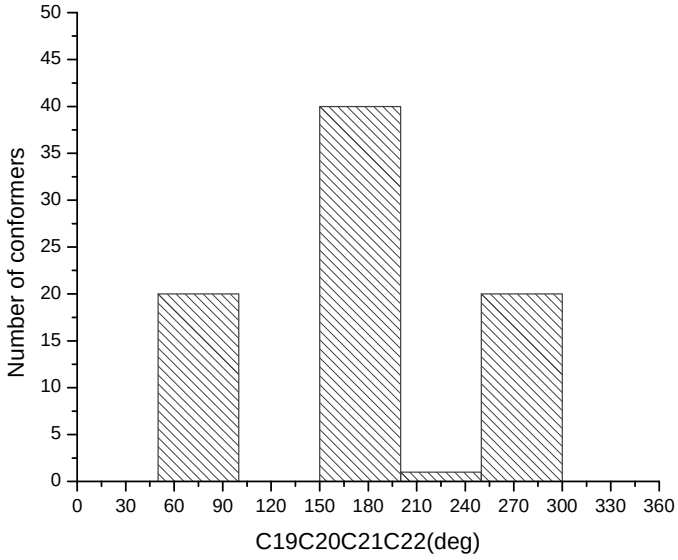

Fig. 24. Histogram of the $C_{19}C_{20}C_{21}C_{22}$ dihedral values in 82 PM3 conformers of PGE2 in a range of 3 kcal/mol

Dihedral $C_{20}C_{21}C_{22}C_{23}$

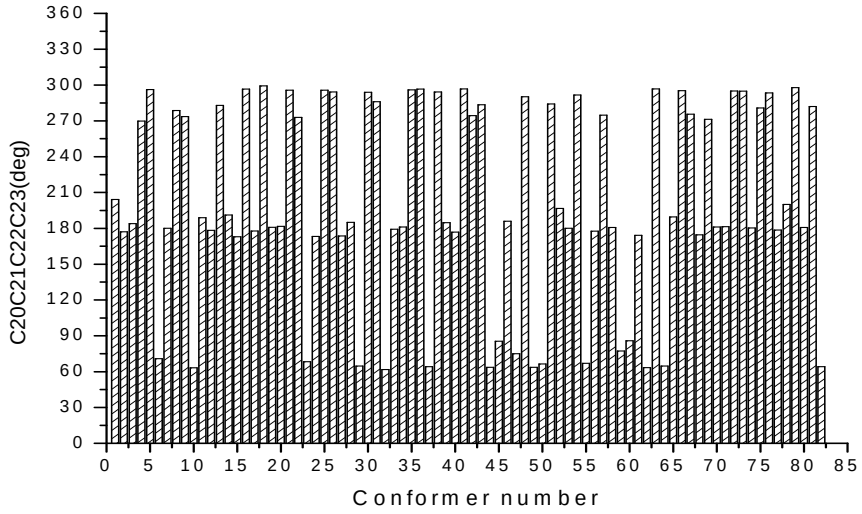

Fig. 25. Values of the $C_{20}C_{21}C_{22}C_{23}$ dihedral in 82 PM3 conformers of PGE2 in a range of 3 kcal/mol

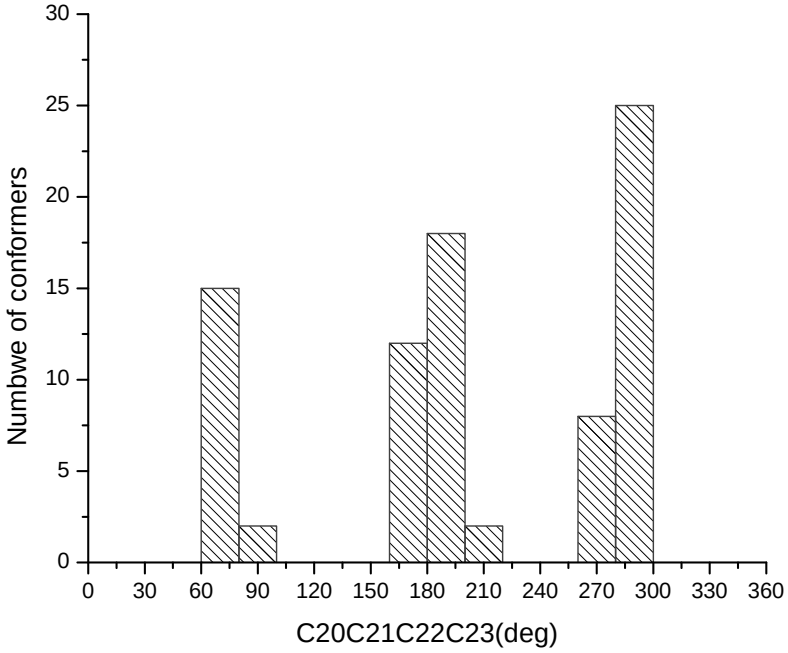

Fig. 26. Histogram of the $C_{20}C_{21}C_{22}C_{23}$ dihedral values in 82 PM3 conformers of PGE2 in a range of 3 kcal/mol

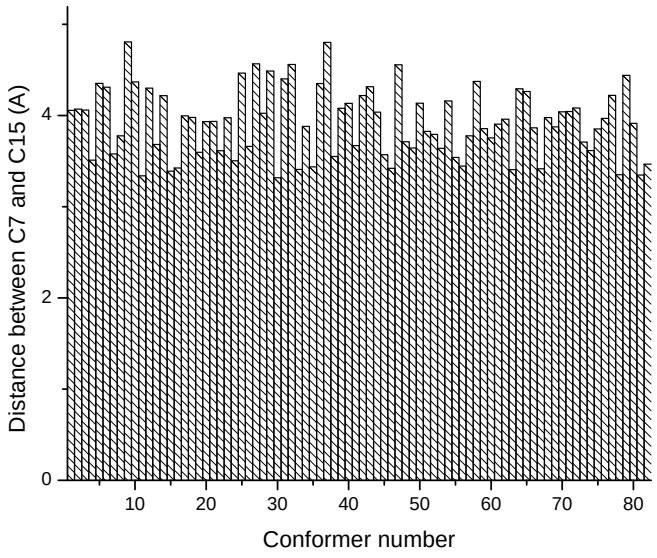

Fig.27. Distribution of distances between the unbounded atoms C_7 and C_{15} in 82 PM3 conformers of PGE2 in a range of 3 kcal/mol

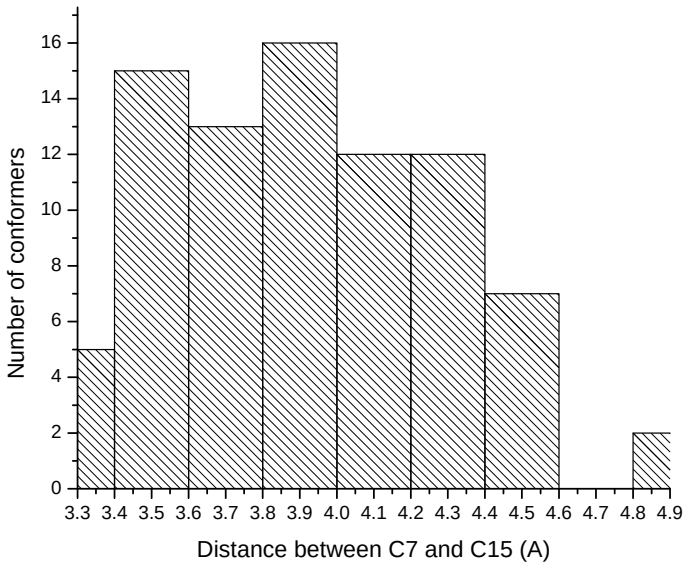

Fig. 28. Histogram of distances between the unbounded atoms C_7 şi C_{15} in 82 PM3 conformers of PGE2 in a range of 3 kcal/mol

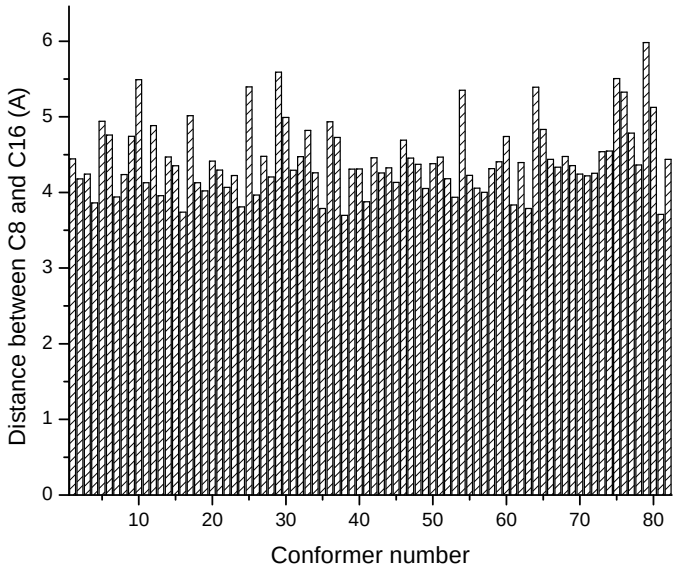

Fig.29. Distribution of distances between the unbounded atoms C_8 and C_{16} in 82 PM3 conformers of PGE2 in a range of 3 kcal/mol

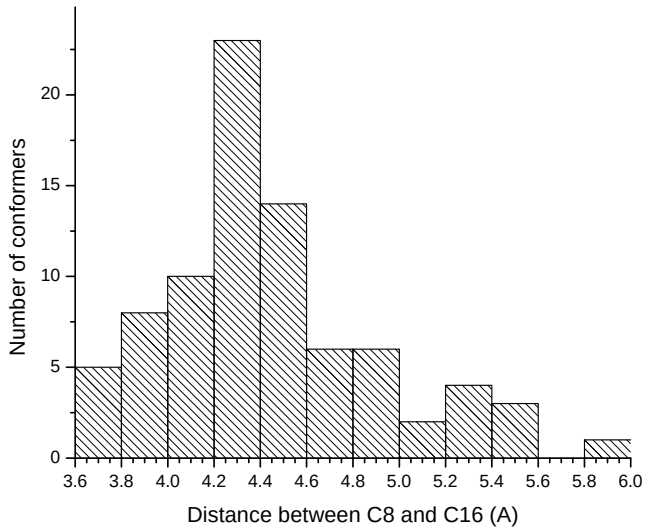

Fig.30. Histogram of distances between the unbounded atoms C_8 and C_{16} in 82 PM3 conformers of PGE2 in a range of 3 kcal/mol

Dihedral $C_{11}C_{12}O_{14}H41$

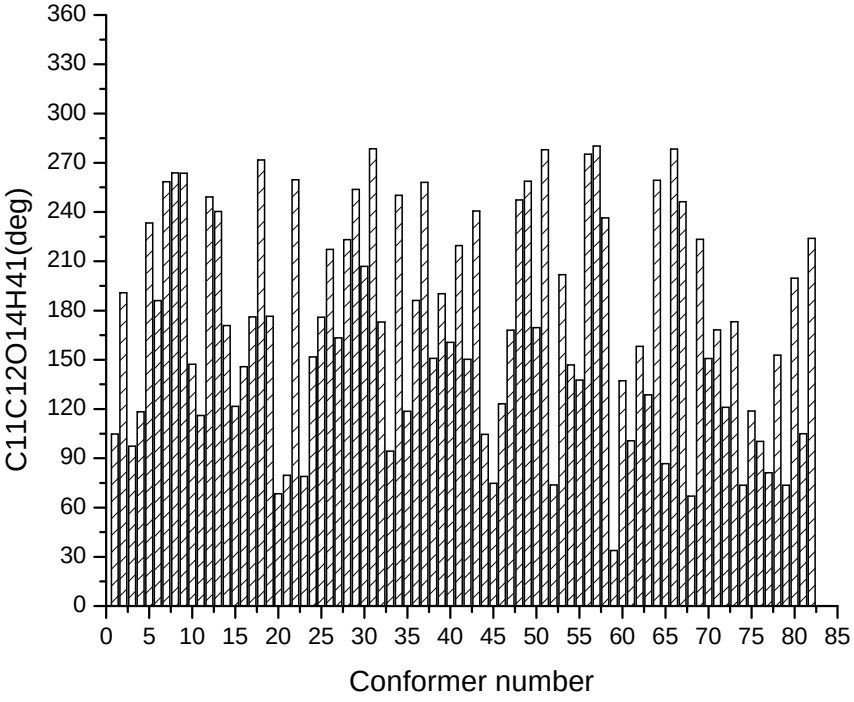

Fig. 31. Values of the $C_{11}C_{12}O_{14}H_{41}$ dihedral in the 82 PM3 conformers of PGE2 in a range of 3 kcal/mol

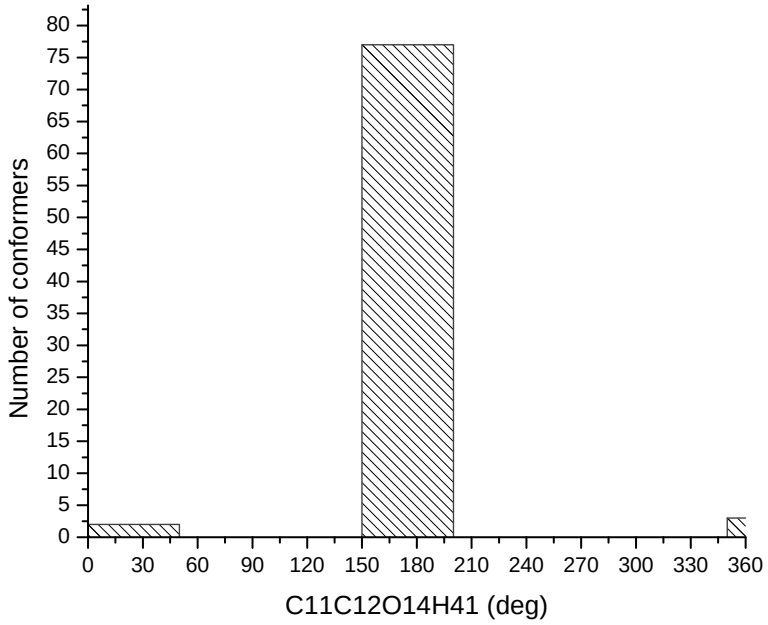

Fig. 32. Histogram of the $C_{11}C_{12}O_{14}H_{41}$dihedral values in 82 PM3 conformers of PGE2 in a range of 3 kcal/mol

B) Molecular dynamics simulations

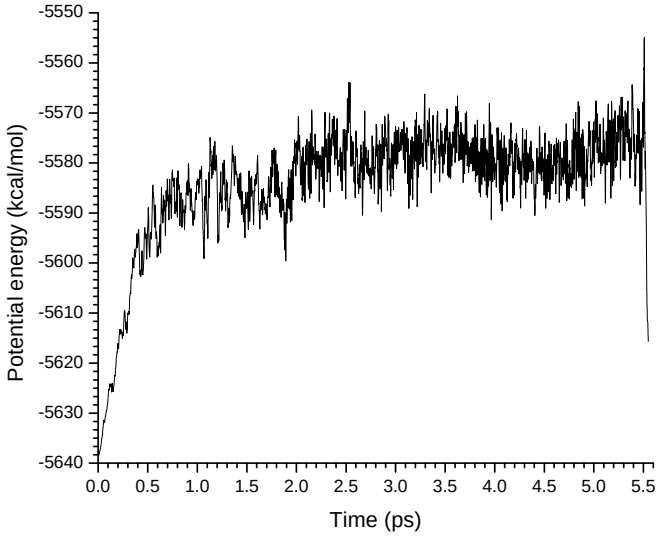

Fig. 33. Variation in time of the PM3 potential energy of the PGE2 conformers resulted from simulated annealing at 400K

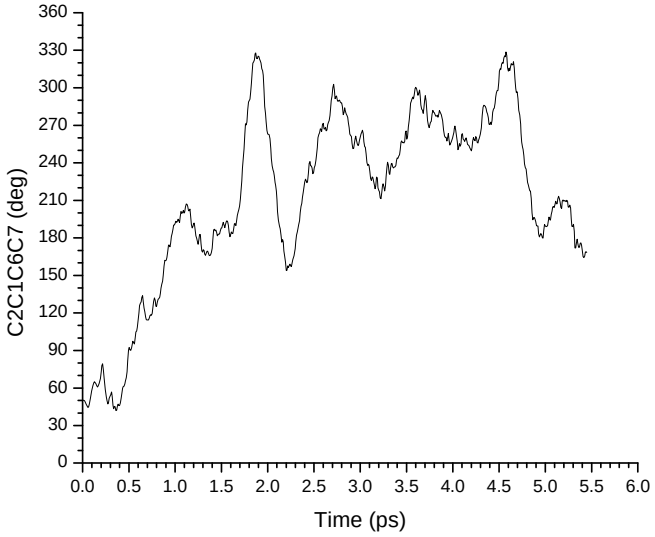

Fig. 34. Variation in time of the $C_2C_1C_6C_7$ dihedral in the PM3 conformers of PGE2 resulted from a simulated annealing run at 400K

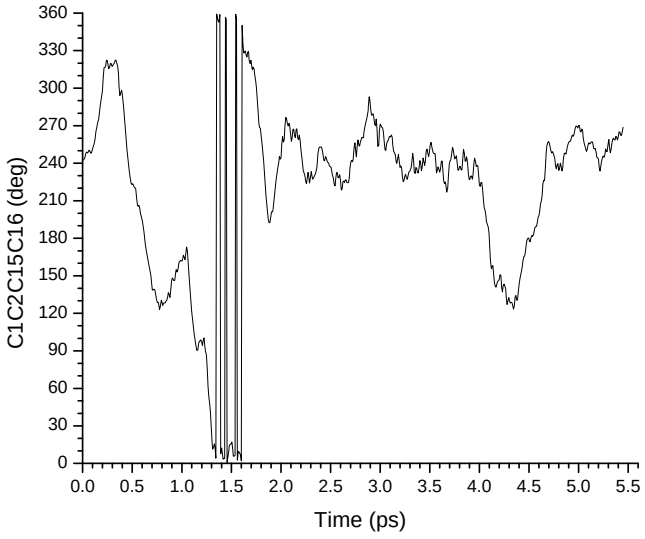

Fig. 35. Variation in time of the $C_1C_2C_{15}C_{16}$ dihedral in the PM3 conformers of PGE2 resulted from a simulated annealing run at 400K

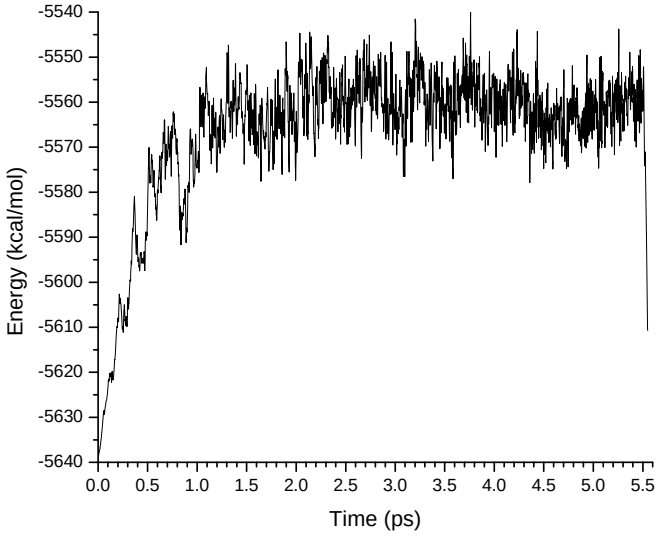

Fig. 36. Variation in time of the PM3 potential energy of the PGE2 conformers resulted from simulated annealing at 600K

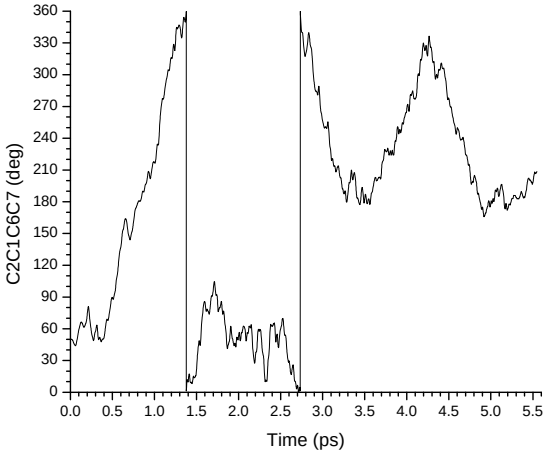

Fig. 37. Variation in time of the $C_2C_1C_6C_7$ dihedral in the PM3 conformers of PGE2 resulted from a simulated annealing run at 600K

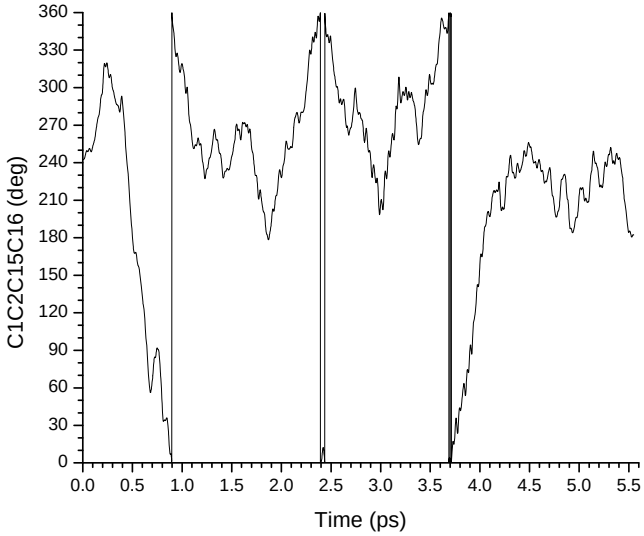

Fig. 38. Variation in time of the $C_1C_2C_{15}C_{16}$ dihedral in the PM3 conformers of PGE2 resulted from a simulated annealing run at 600K

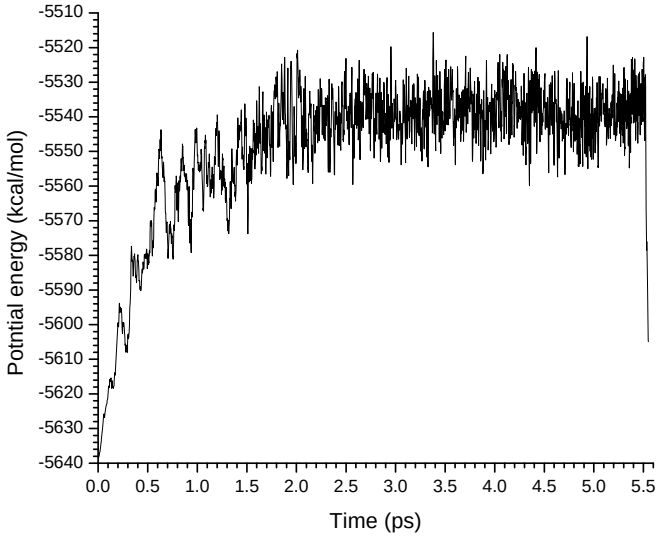

Fig. 39. Variation in time of the PM3 potential energy of the PGE2 conformers resulted from simulated annealing at 800K

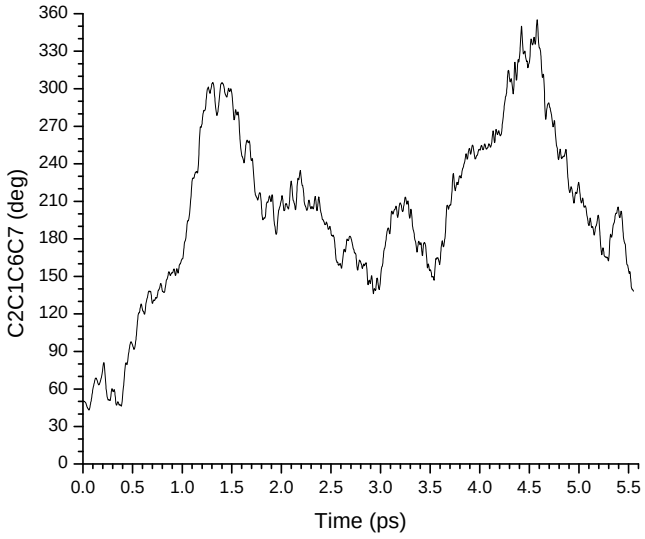

Fig. 40. Variation in time of the $C_2C_1C_6C_7$ dihedral in the PM3 conformers of PGE2 resulted from a simulated annealing run at 800K

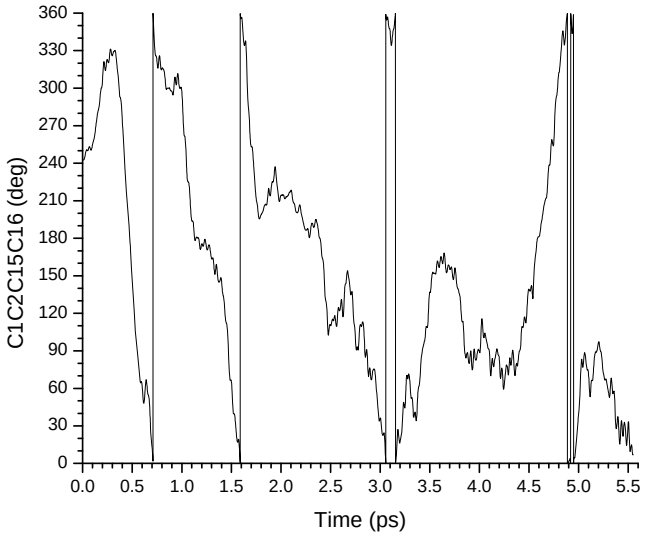

Fig. 41. Variation in time of the $C_1C_2C_{15}C_{16}$ dihedral in the PM3 conformers of PGE2 resulted from a simulated annealing run at 800 K

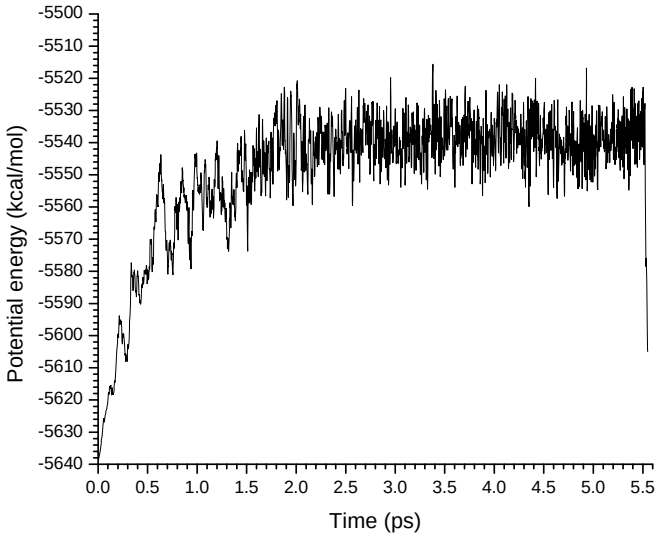

Fig. 42. Variation in time of the PM3 potential energy of the PGE2 conformers resulted from simulated annealing at 1000K

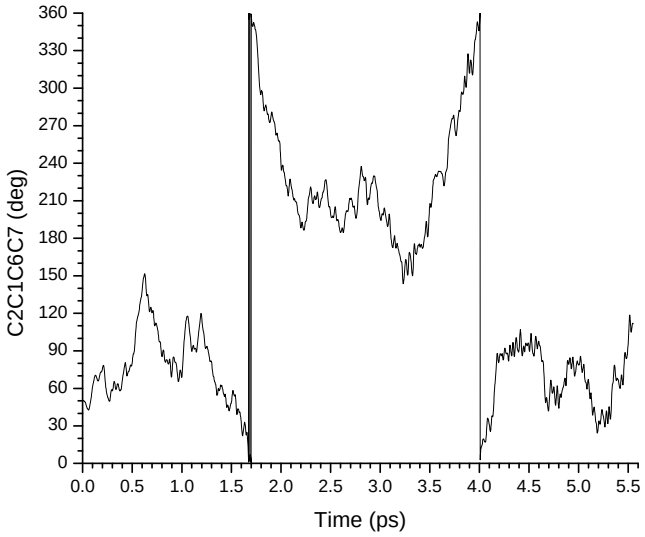

Fig. 43. Variation in time of the $C_2C_1C_6C_7$ dihedral in the PM3 conformers of PGE2 resulted from a simulated annealing run at 1000 K

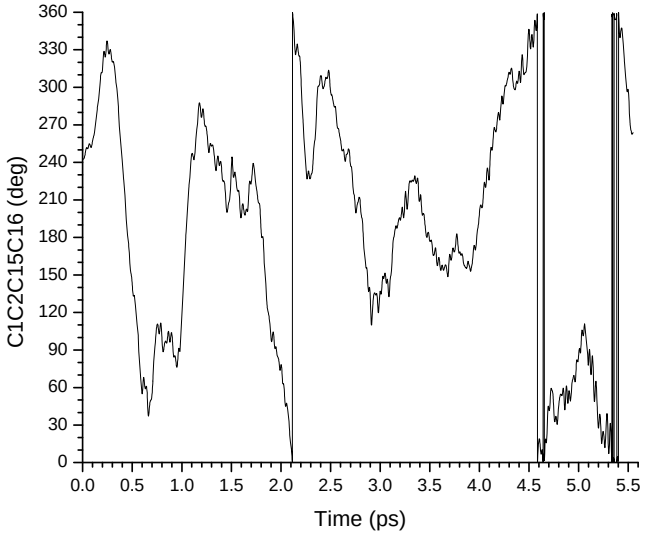

Fig. 44. Variation in time of the $C_1C_2C_{15}C_{16}$ dihedral in the PM3 conformers of PGE2 resulted from a simulated annealing run at 1000 K

C) **Potential energy profiles** are shown on two scales
a) one containing all energy range and
b) the other containing only energy values up to 25 kcal/mol.
The differnces between the energy of each conformer and the one of the global minimum conformer (-5638.42 kcal/mol) are plotted against the dihedral values.

Bond C1-C5

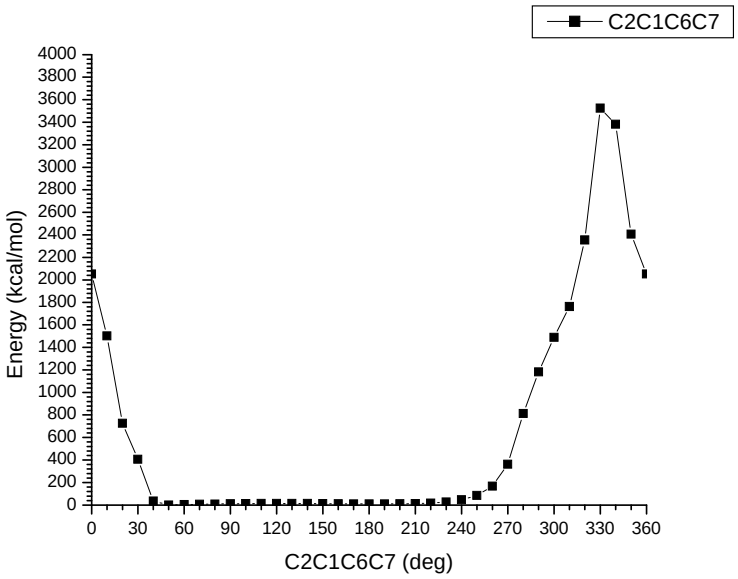

(a)

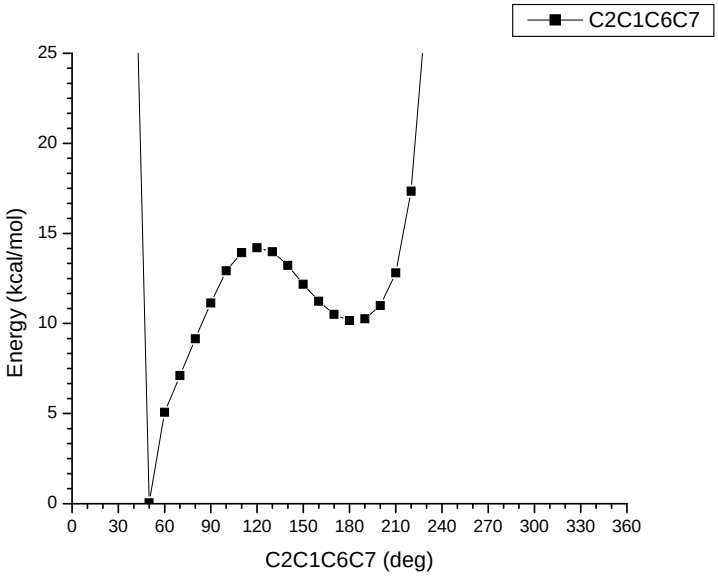

(b)

Fig. 45. Potential energy profile for the C1-C6 bond rotation

C6-C7 bond

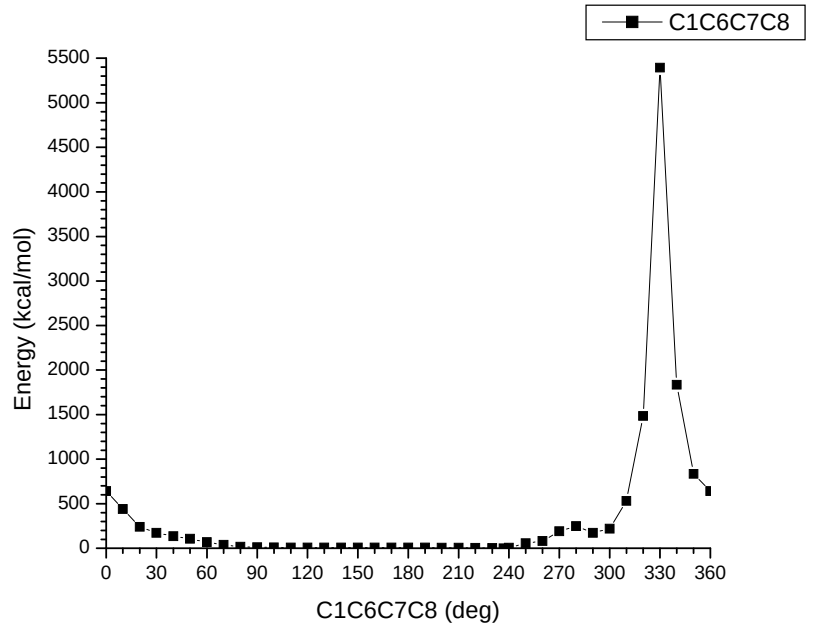

(a)

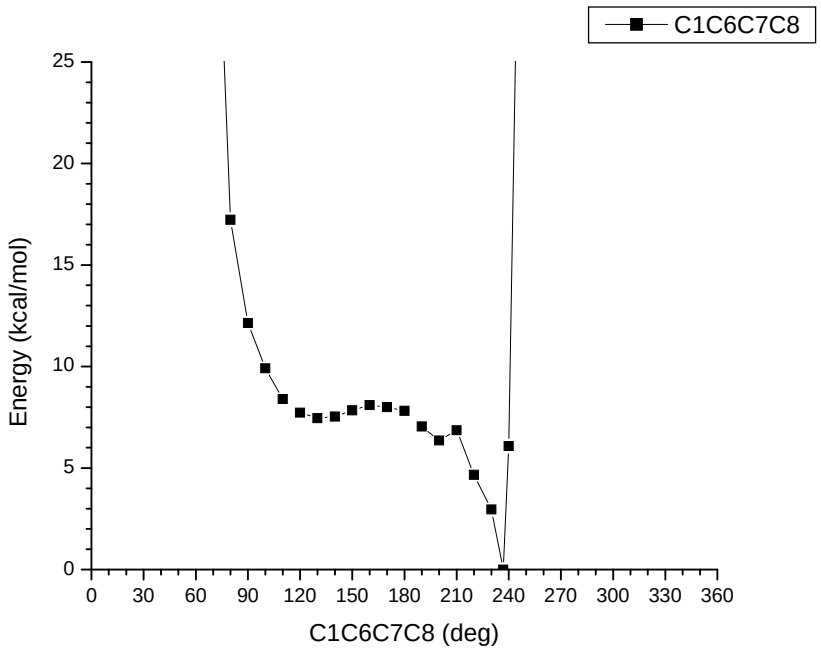

(b)

Fig. 46. Potential energy profile for the C6-C7 bond rotation

C8-C9 bond

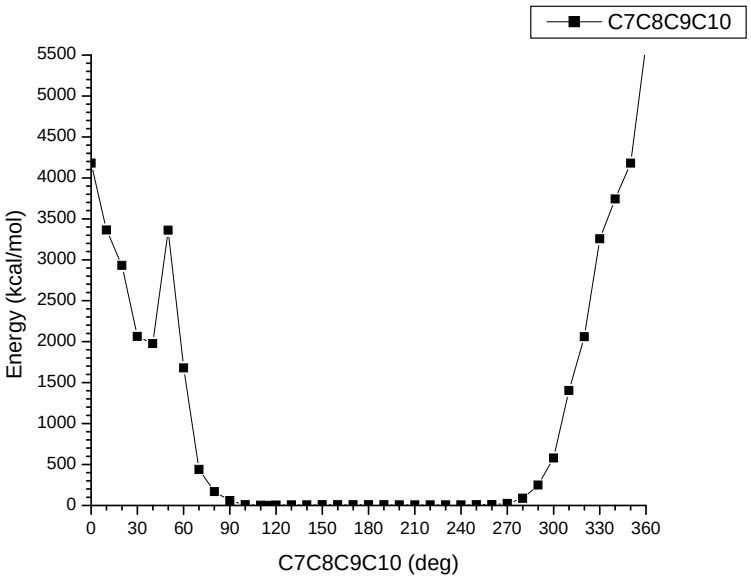

(a)

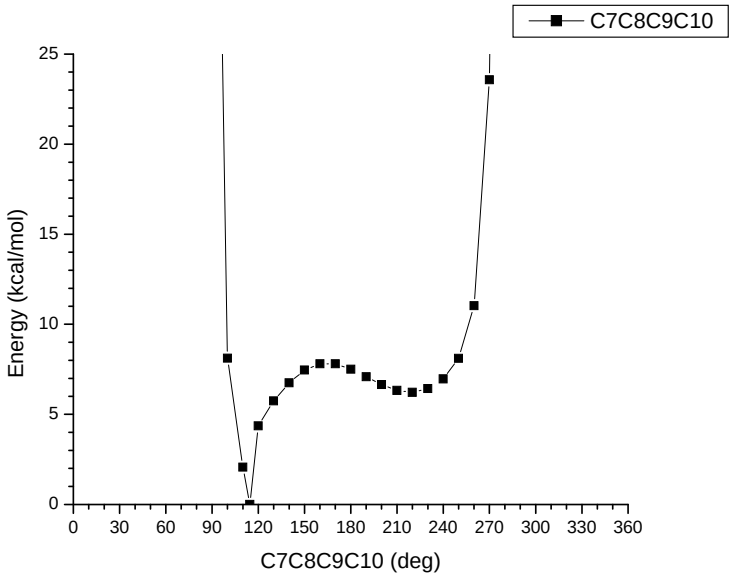

(b)

Fig. 47. Potential energy profile for the C8-C9 bond rotation

C9-C10 bond

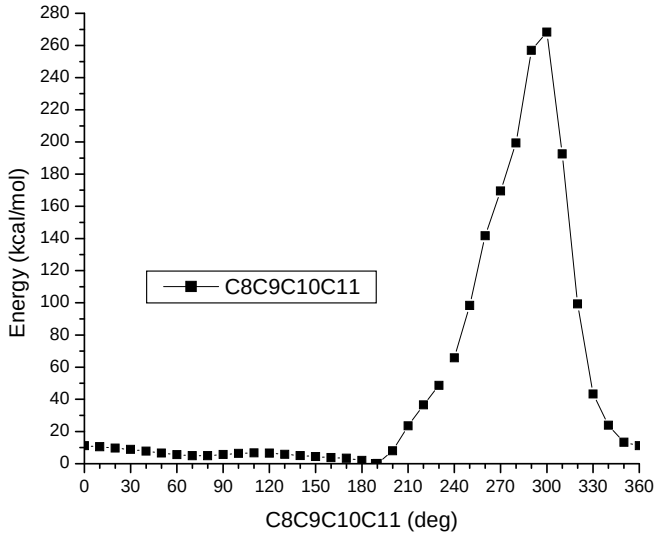

1

(a)

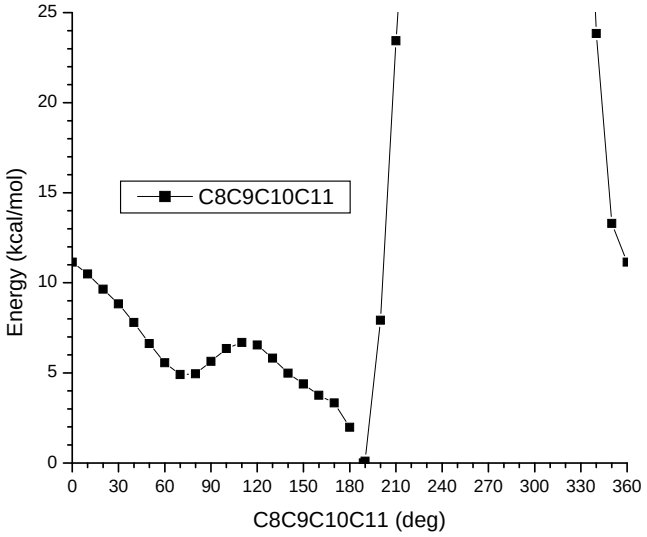

(b)

Fig. 48. Potential energy profile for the C9-C10 bond rotation

C10-C11 bond

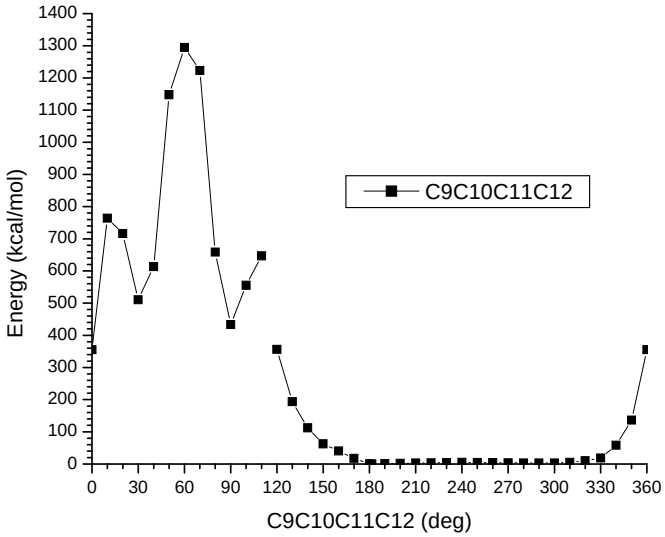

(a)

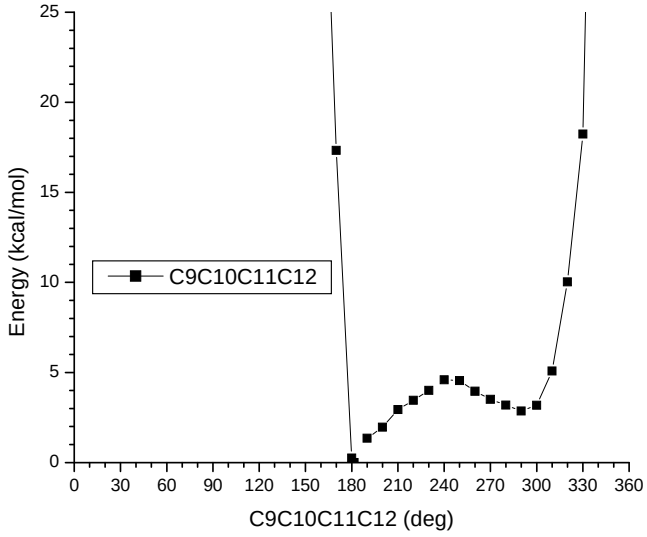

(b)

Fig. 49. Potential energy profile for the C10-C11 bond rotation

C2-C15 bond

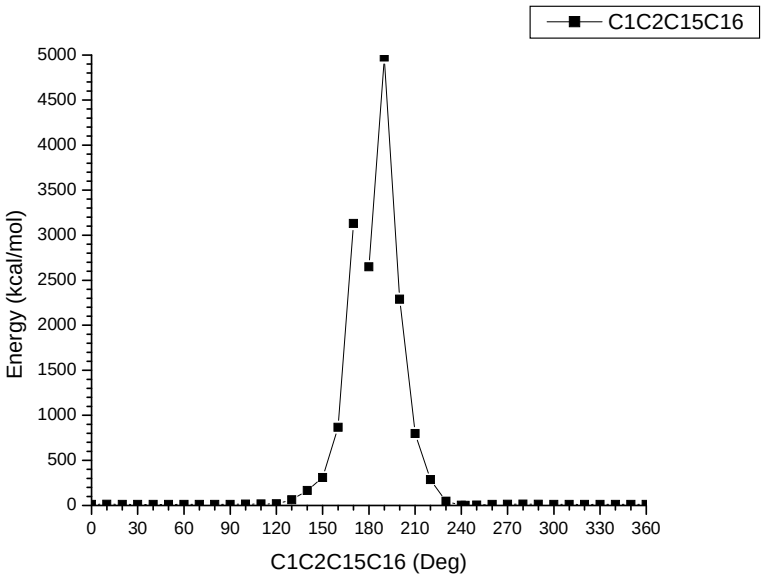

(a)

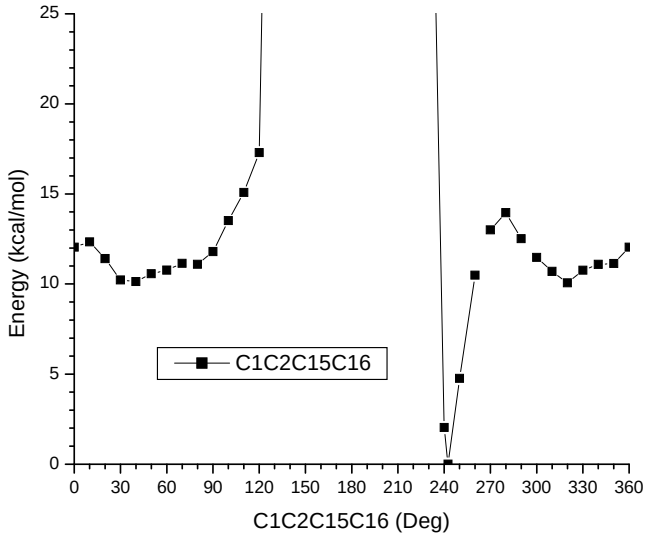

(b)

Fig. 50. Potential energy profile for the C2-C15 bond rotation

C16-C17 bond

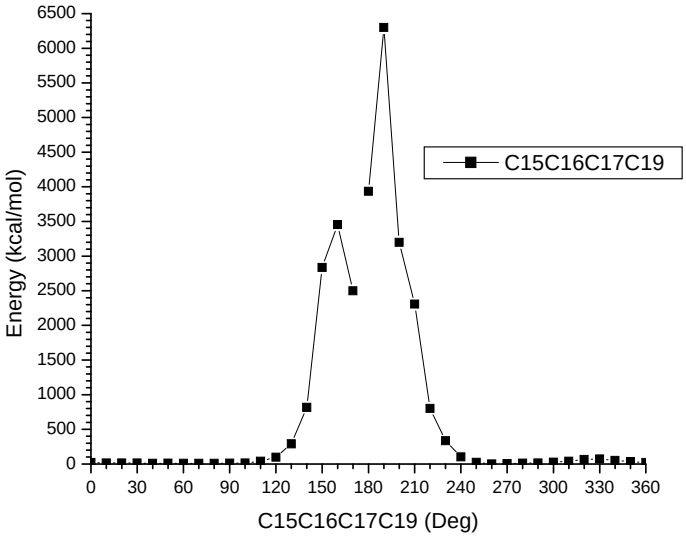

(a)

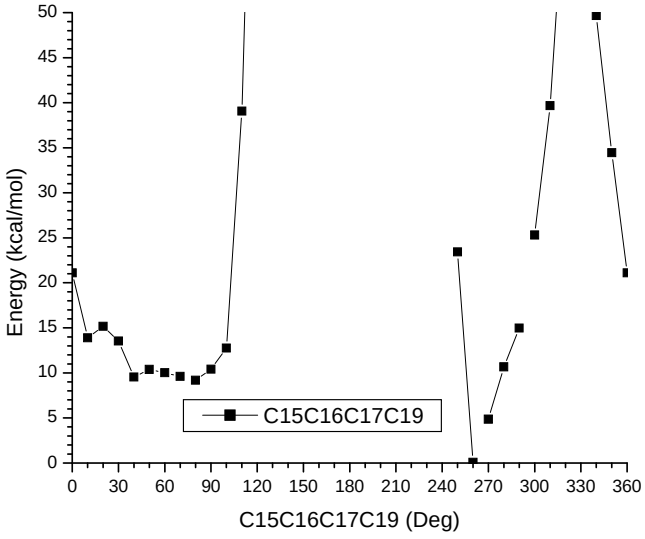

(b)

Fig. 51. Potential energy profile for the C16-C17 bond rotation

C17-C19 bond

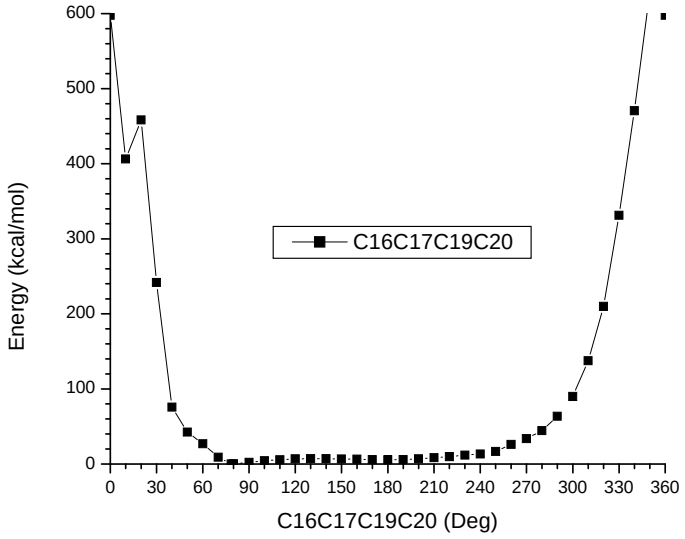

(a)

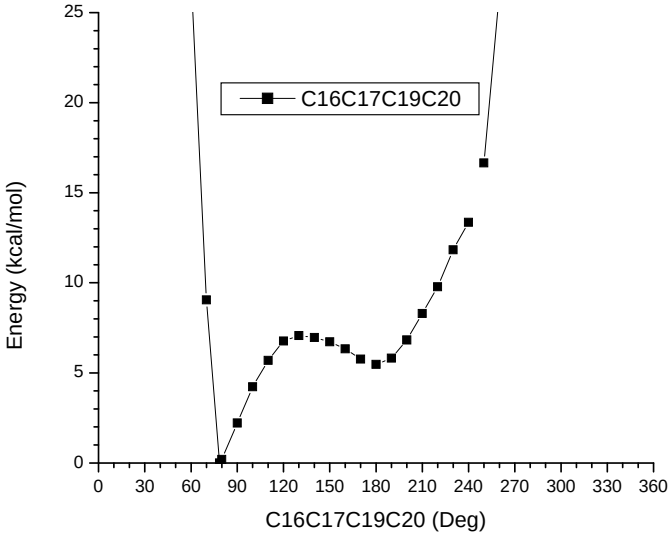

(b)

Fig. 52. Potential energy profile for the C17-C19 bond rotation

C19-C20 bond

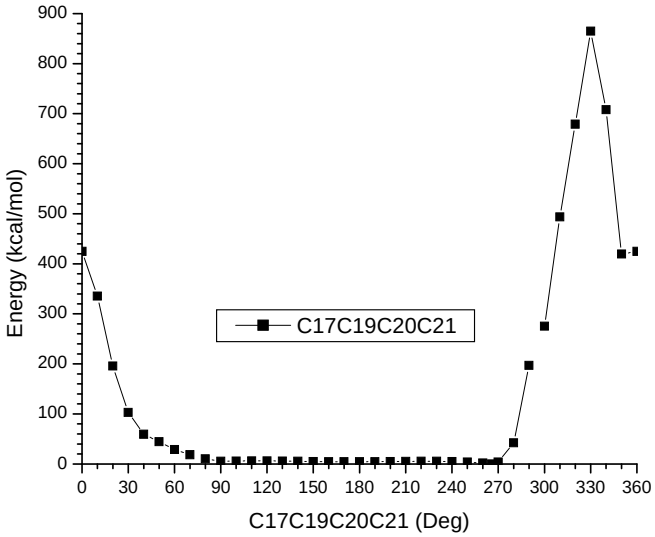

(a)

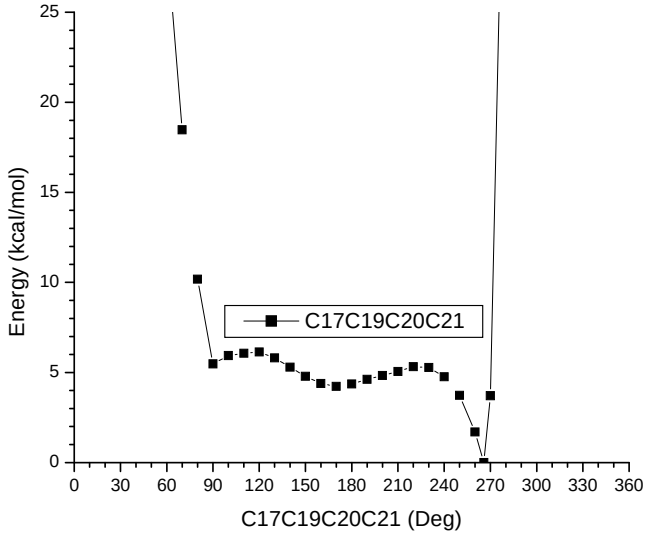

(b)

Fig. 53. Potential energy profile for the C19-C20 bond rotation

C20-C21 bond

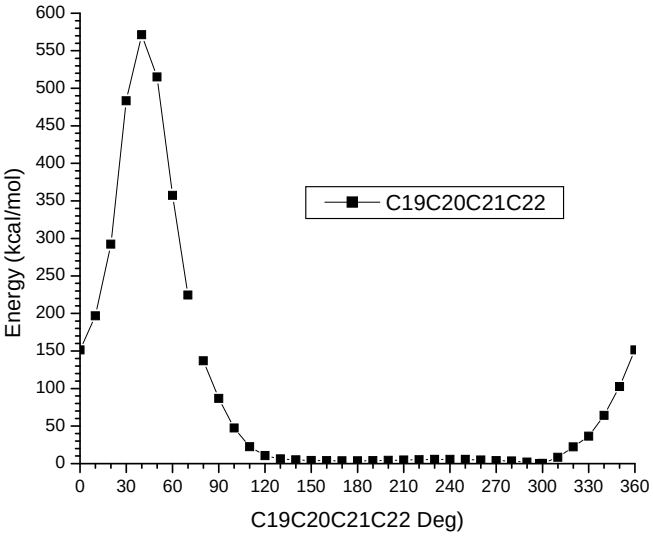

(a)

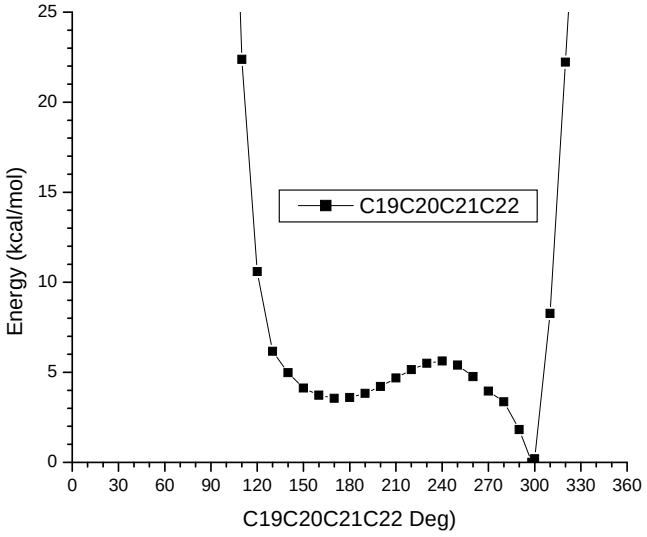

(b)

Fig. 54. Potential energy profile for the C20-C21 bond rotation

C21-C22 bond

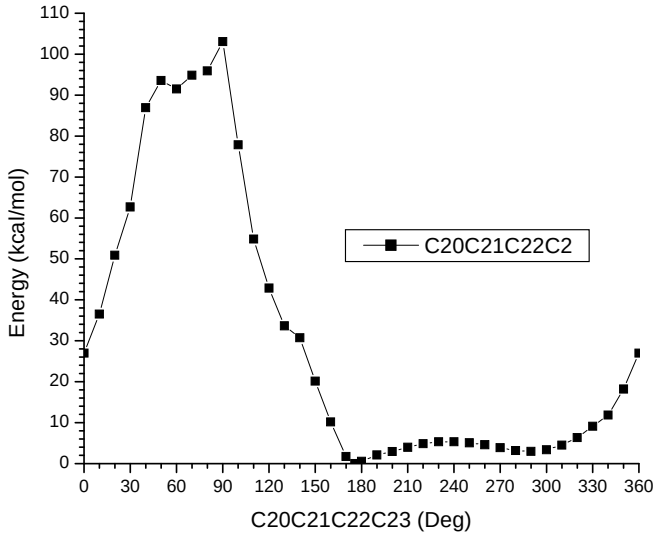

(a)

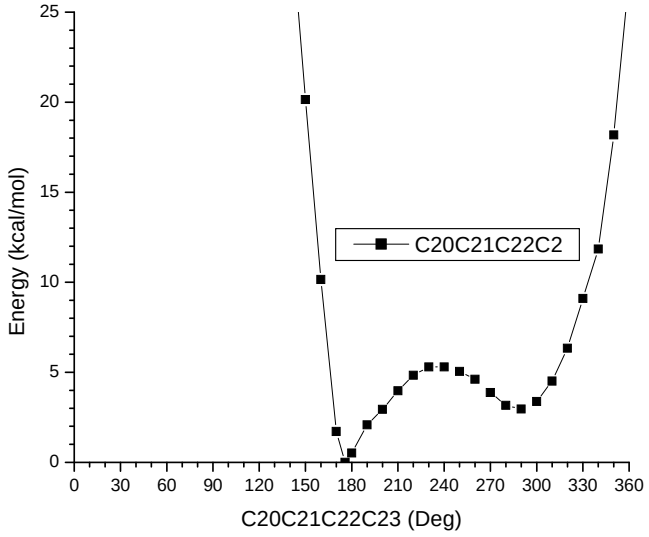

(b)

Fig. 55. Potential energy profile for the C21-C22 bond rotation

D) Comparisons of potential energy profiles resulted through the rotation of the flexible bonds in each substituent

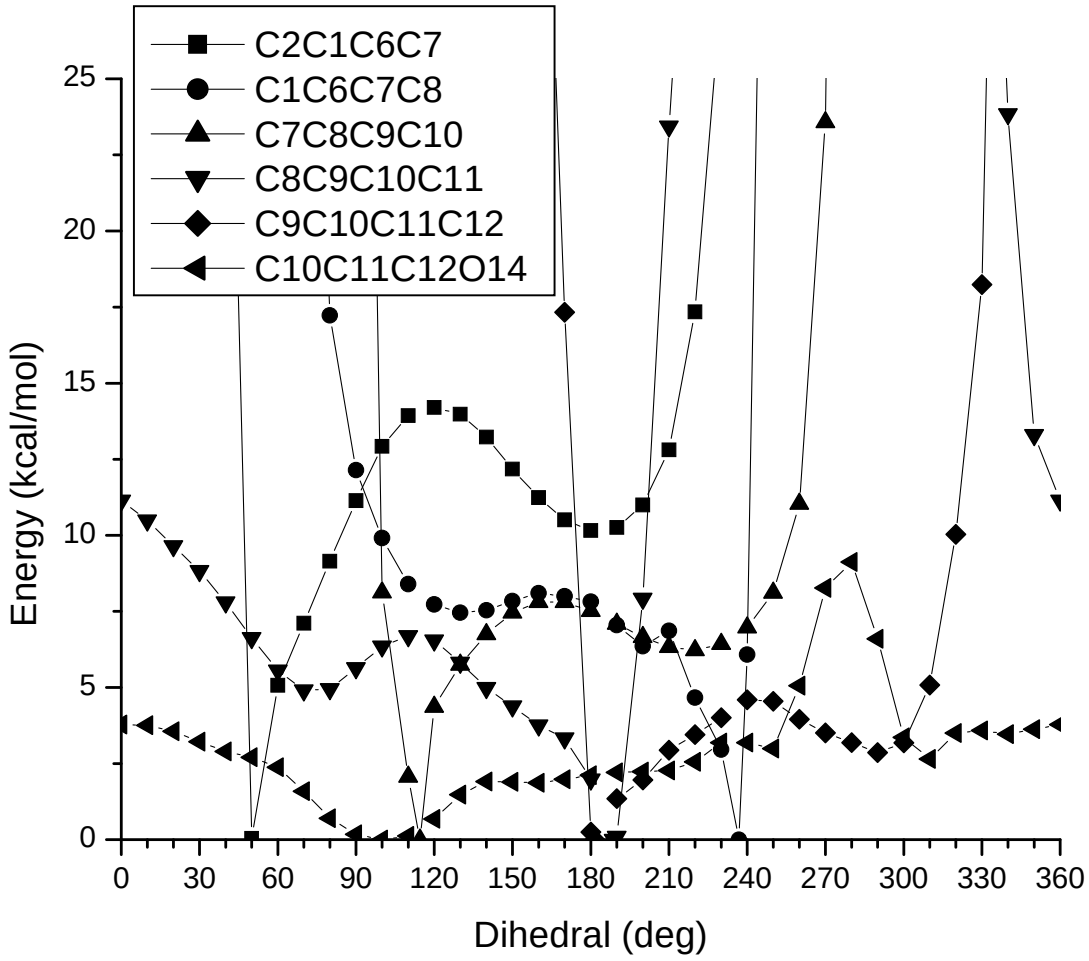

Fig 56. PM3 potential energy profiles for the PGE2 conformer interconversion to the rotation of flexible bonds in the substituent (Z)-hept-5-enoic acid. Energy is plotted against the energy of the conformer in the global minim (-5638.42 kcal/mol) taken as zero. Only energy values up to 25 kcal/mol are plotted.

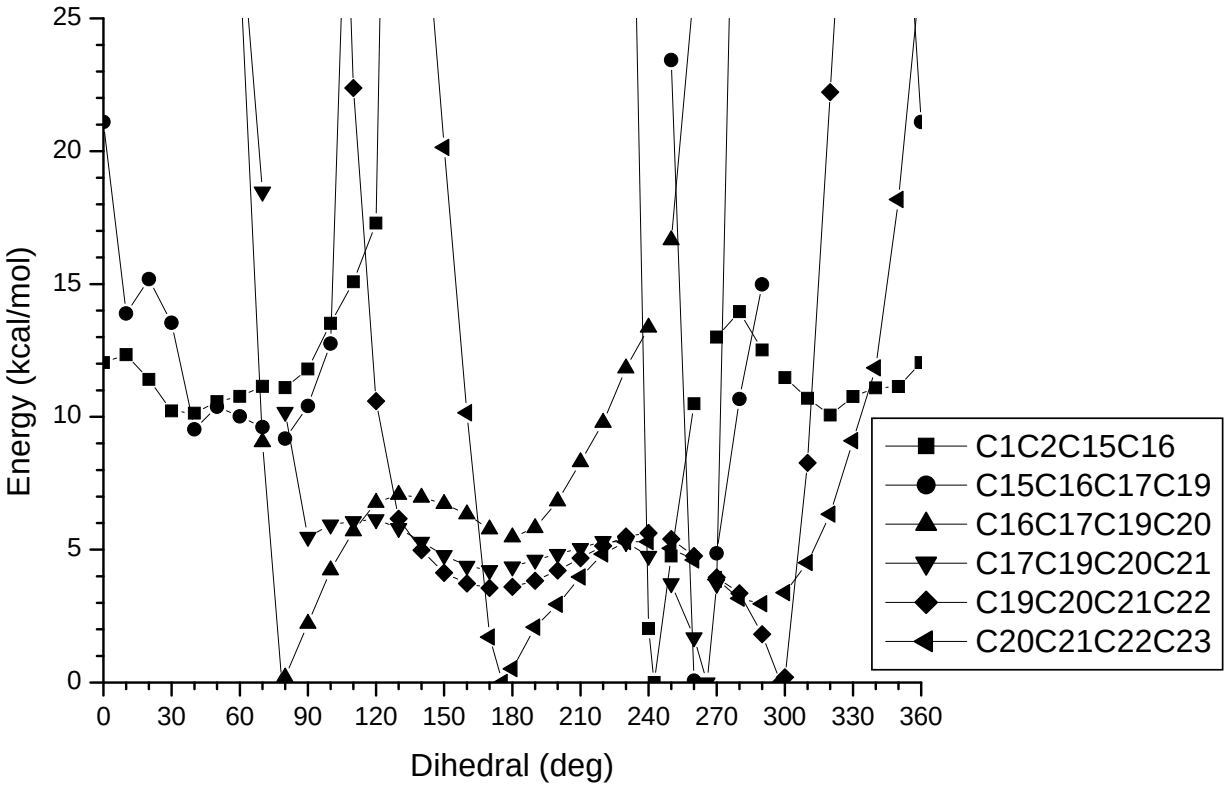

Fig 57. PM3 potential energy profiles for the PGE2 conformer interconversion to the rotation of flexible bonds in the substituent (E)-(S)-oct-1-en-3-ol. Energy values are plotted against the energy of the conformer from the global minim (-5638.42 kcal/mol) taken as zero.

E) Conformers and superpositions of different conformers with the global minimum conformer or the conformer docked in a 3D model of the human EP4 receptor.

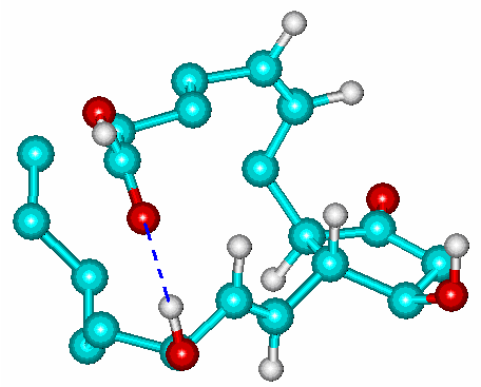

Fig. 58. Global minimum conformer and the intramolecular H bond between O_{13} atom from the carboxyl group and H_{45} atom from the $O_{18}H_{45}$ group.

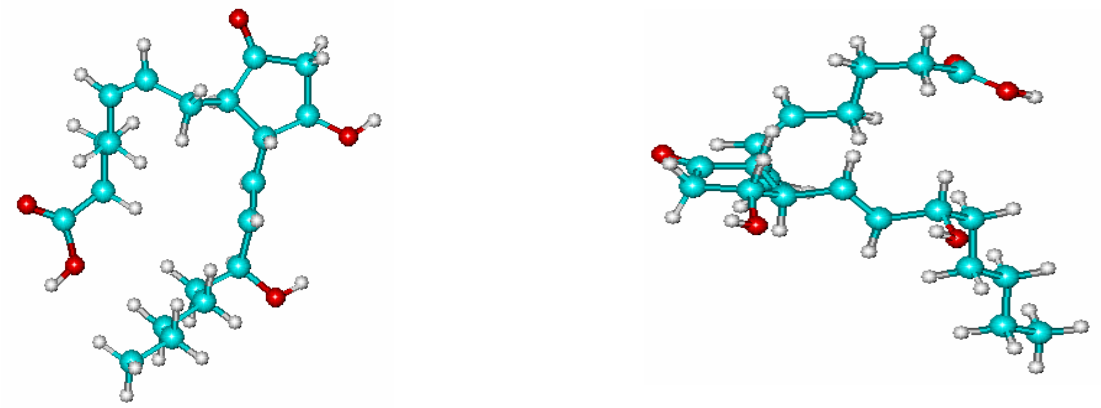

Fig. 59. Two different views of the conformer docked in the binding site of the 3D model of the EP4 receptor.

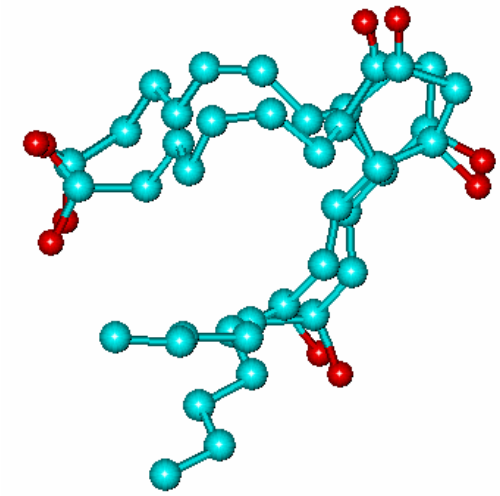

Fig. 60. Superposition of the conformer docked in the 3D model of the EP4 receptor and the PM3 conformer which gives the least distances between the corresponding oxygen atoms from the two conformers.